(12) **United States Patent**
Ho et al.

(10) **Patent No.:** **US 7,511,870 B2**
(45) **Date of Patent:** **Mar. 31, 2009**

(54) **HIGHLY TUNABLE LOW-IMPEDANCE CAPACITIVE MICROMECHANICAL RESONATORS, OSCILLATORS, AND PROCESSES RELATING THERETO**

(75) Inventors: **Gavin Kar-Fai Ho**, Vancouver (CA); **Farrokh Ayazi**, Smyrna, GA (US); **Siavash Pourkamali**, Atlanta, GA (US); **Krishnakumar Sundaresan**, Smyrna, GA (US)

(73) Assignee: **Georgia Tech Research Corp.**, Atlanta, GA (US)

(*) Notice: Subject to any disclaimer, the term of this patent is extended or adjusted under 35 U.S.C. 154(b) by 162 days.

(21) Appl. No.: **11/251,197**

(22) Filed: **Oct. 15, 2005**

(65) **Prior Publication Data**

US 2006/0125576 A1 Jun. 15, 2006

Related U.S. Application Data

(60) Provisional application No. 60/619,739, filed on Oct. 18, 2004.

(51) **Int. Cl.**

G02B 26/00	(2006.01)
H03H 9/00	(2006.01)
H01L 41/00	(2006.01)

(52) **U.S. Cl.** **359/237**; 333/186; 310/314

(58) **Field of Classification Search** .... 73/504.03, 73/514.37, 514.38, 514.32, 862.59, 504.12, 73/504.14, 504.15, 105; 310/309, 321, 324, 310/330–332, 366, 314, 317, 320, 353; 333/186, 333/197, 200; 331/108 C, 116 R, 158; 359/631, 359/290, 291

See application file for complete search history.

(56) **References Cited**

U.S. PATENT DOCUMENTS

6,230,563	B1 *	5/2001	Clark et al.	73/504.04
6,236,281	B1 *	5/2001	Nguyen et al.	331/154
6,630,871	B2 *	10/2003	Ma et al.	331/116 M
2006/0273416	A1 *	12/2006	Ayazi et al.	257/414

OTHER PUBLICATIONS

S. Lee, M.U. DeMirci and C. Nguyen, "A 10-MHz micromechanical resonator Pierce reference oscillator," Tech. Dig. Transducers 01, pp. 1094-1098, 2001.

S. Pourkamali, Z. Hao, and F. Ayazi, "VHF Single Crystal Silicon Capacitive Elliptic Bulk-Mode Disk Resonators," published in JMEMS, V13 N6, 2004.

(Continued)

Primary Examiner—Ricky L Mack
Assistant Examiner—Tuyen Q Tra
(74) *Attorney, Agent, or Firm*—Kenneth W. Float

(57) **ABSTRACT**

Disclosed are capacitive micromechanical resonators optimized for high Q, low motional impedance, and large tuning range. Exemplary resonators were fabricated using a HARPSS-on-SOI process, and demonstrated quality factors up to 119000 in vacuum. For resonators operating between 3 MHz and 30 MHz, the lowest extracted impedance is 218 kΩ and the largest electrostatic tuning coefficient is −240 ppm/V^2. The disclosed designs are applicable up to at least 200 MHz operation. An oscillator interface circuit comprising of a trans-impedance amplifier and an automatic bias generator providing a temperature-compensating bias voltage is also disclosed. Experiments show temperature drift reduction from 2800 ppm to 39 ppm over a 100° C. range. Process compensation (DFM) of micromechanical resonators, resonators having mass loading elements that allow generation of closely spaced frequencies, and coupled systems comprising of the resonators are also described.

21 Claims, 11 Drawing Sheets

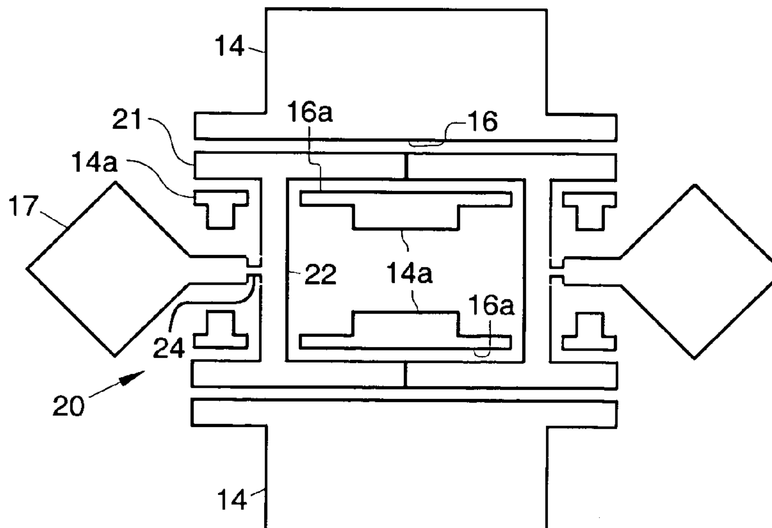

OTHER PUBLICATIONS

S. Pourkamali, G. K. Ho, F. Ayazi, "Vertical Capacitive SiBARs," published in Proc. IEEE MEMS'05, Jan. 30-Feb. 3, 2005, pp. 211-214.

S. Pourkamali, et al., "Fully single crystal silicon resonators with deep-submicron dry-etched transducer gaps", in Proc. IEEE MEMS '04, The Netherlands, Jan. 2004, pp. 813-816.

* cited by examiner

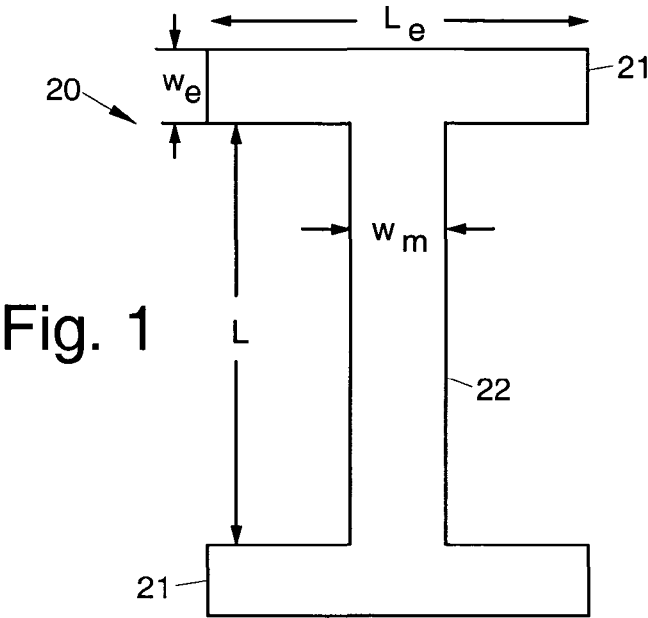

Fig. 1

L_e = electrode/flange length
w_e = flange width
L = rod length
w_m = rod width
h = device thickness
V_p = polariation voltage
Q = quality factor
ε = free space permittivity
d = capacitive gap size

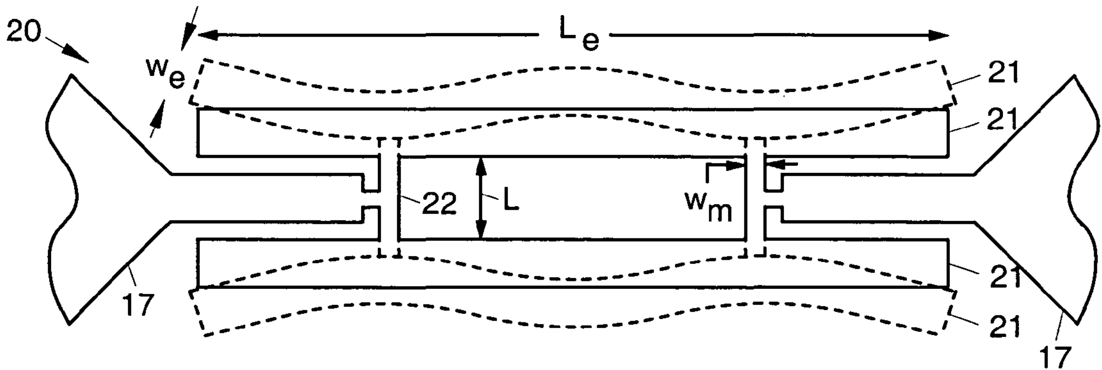

Fig. 2

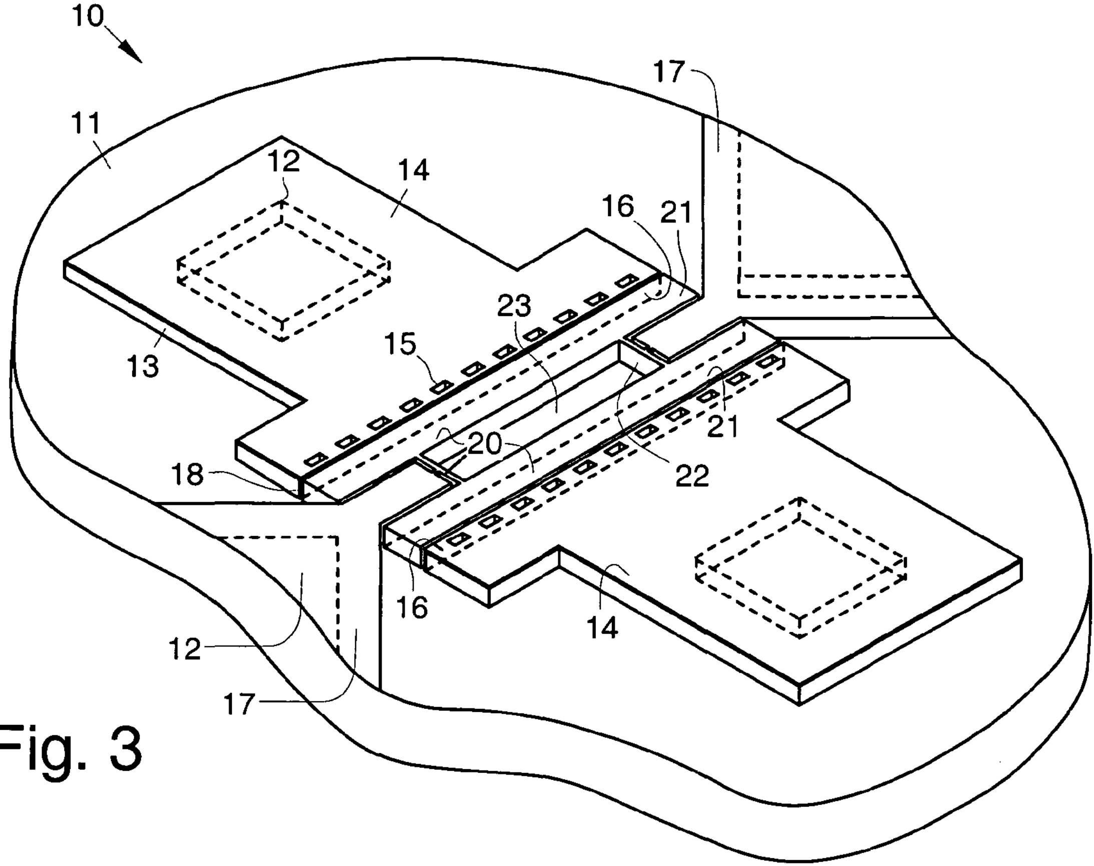

Fig. 3

Fig. 3a

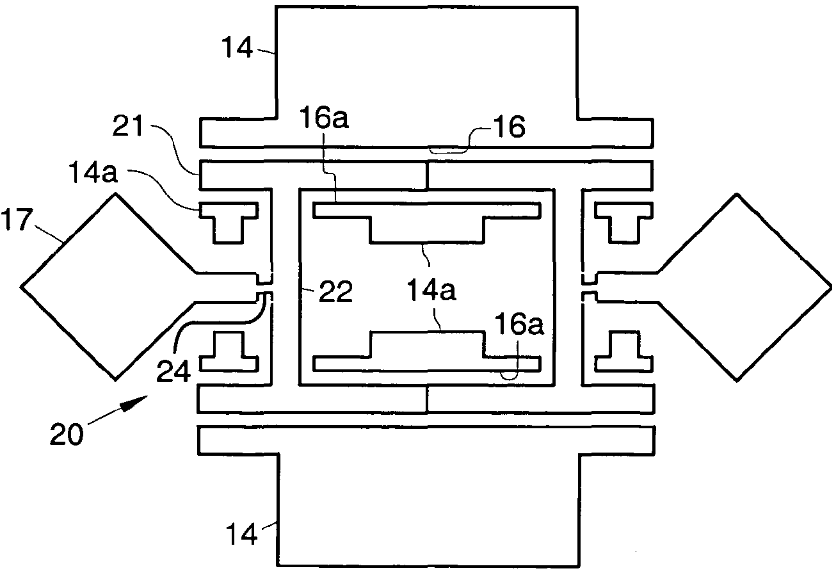

Fig. 4

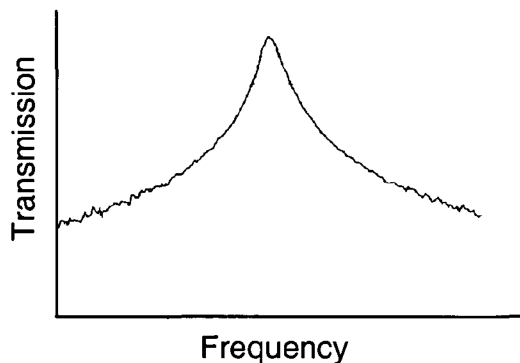

Fig. 5

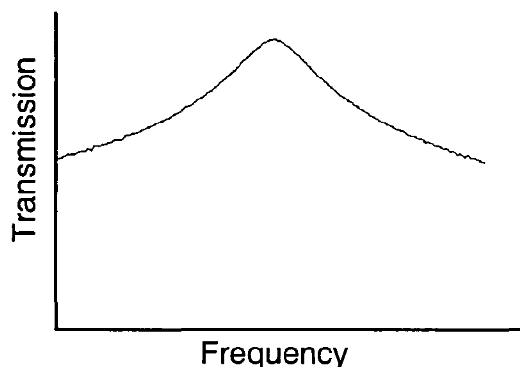

Fig. 6

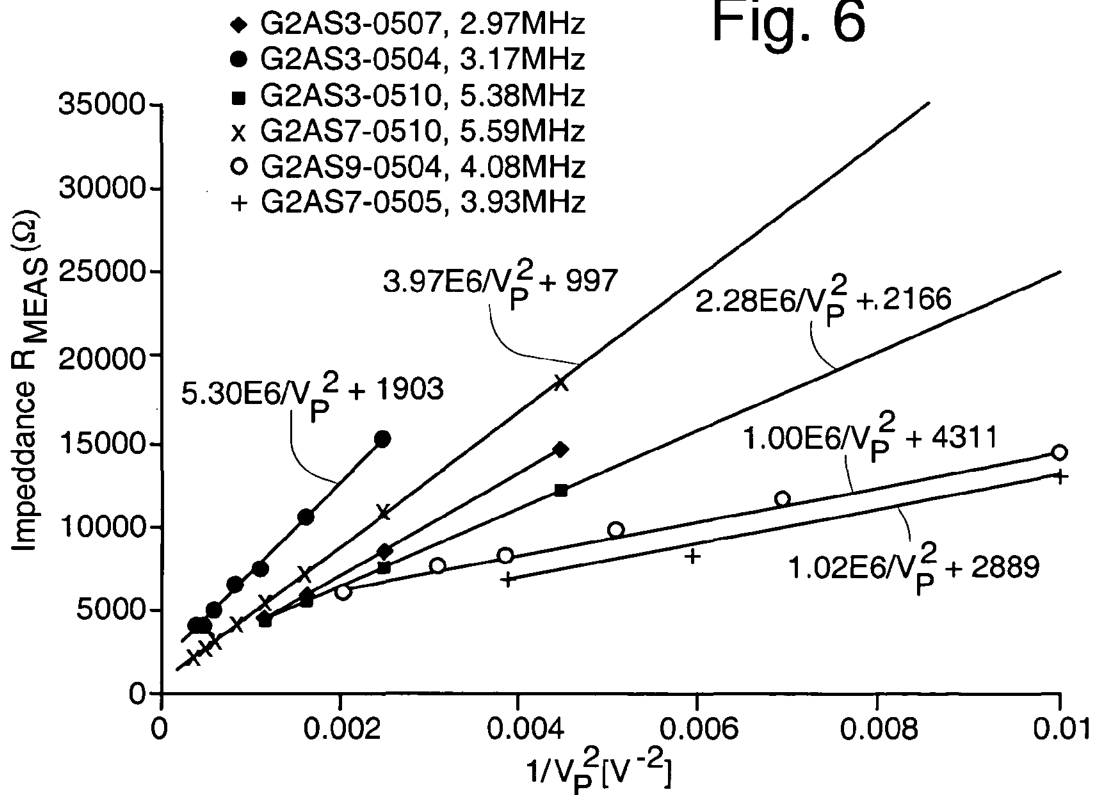

Fig. 7

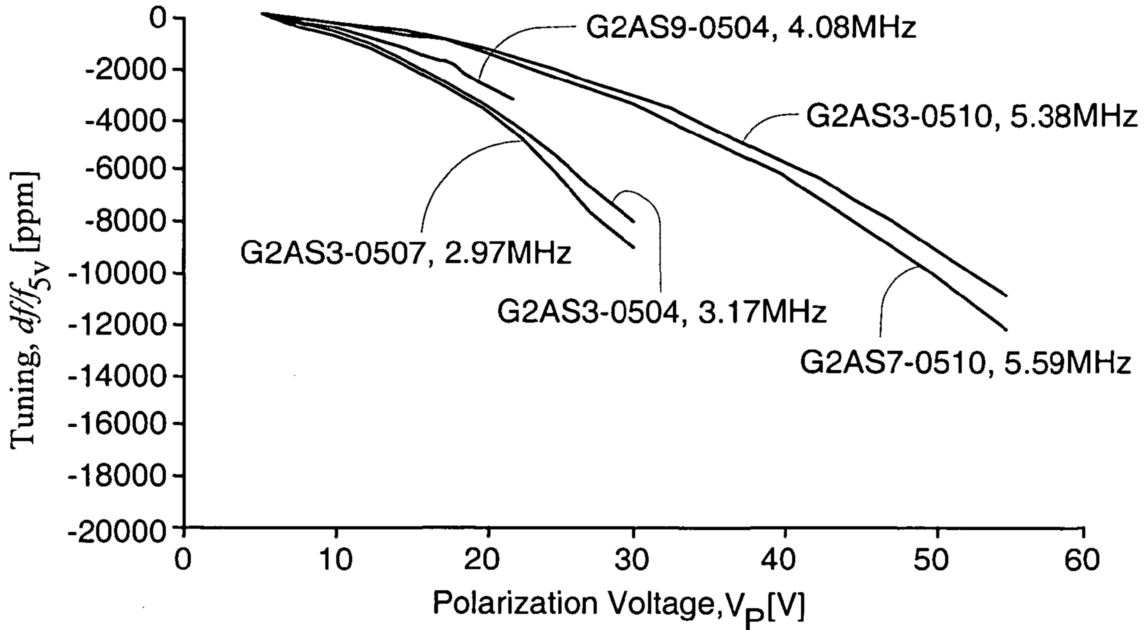

Fig. 7a

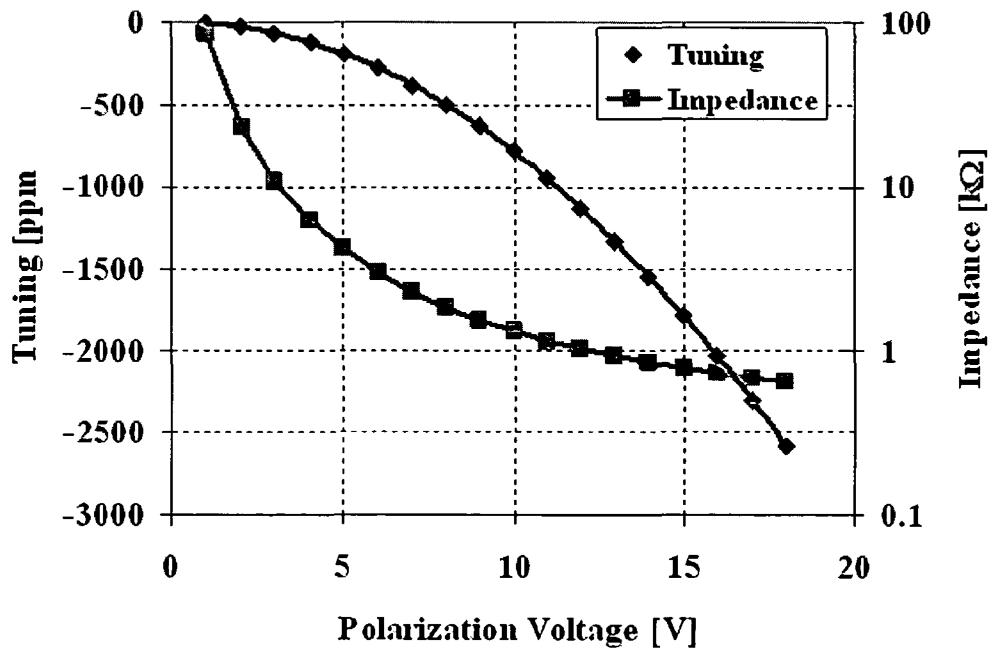

Fig. 7b

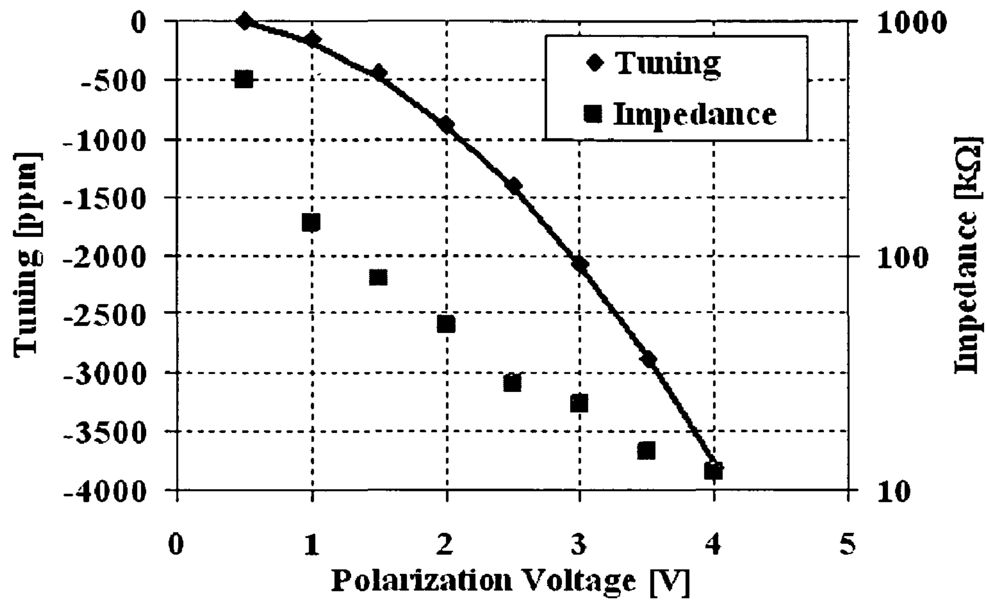

Fig. 7c

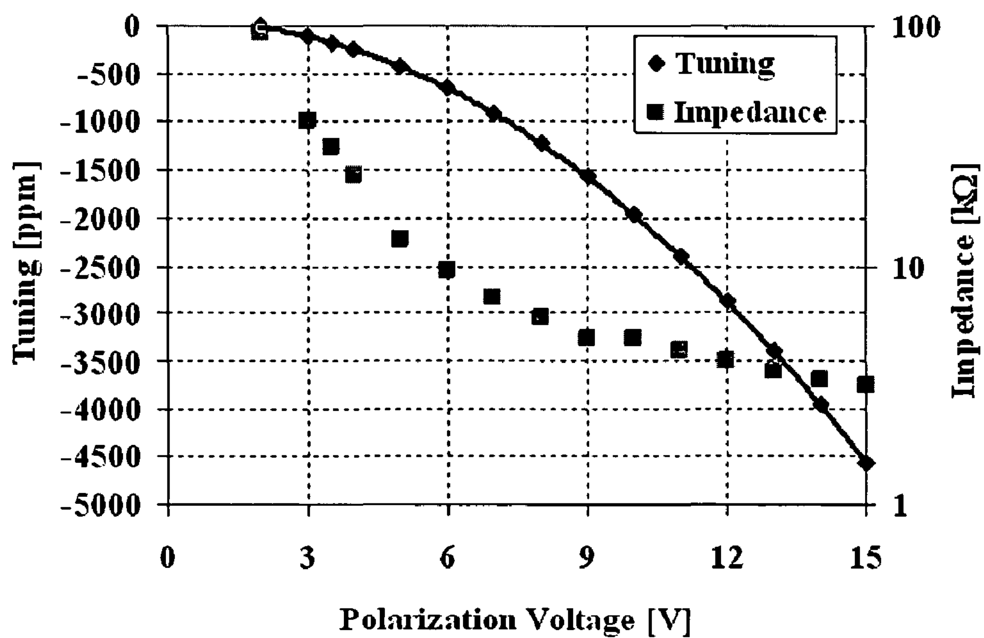

Fig. 8

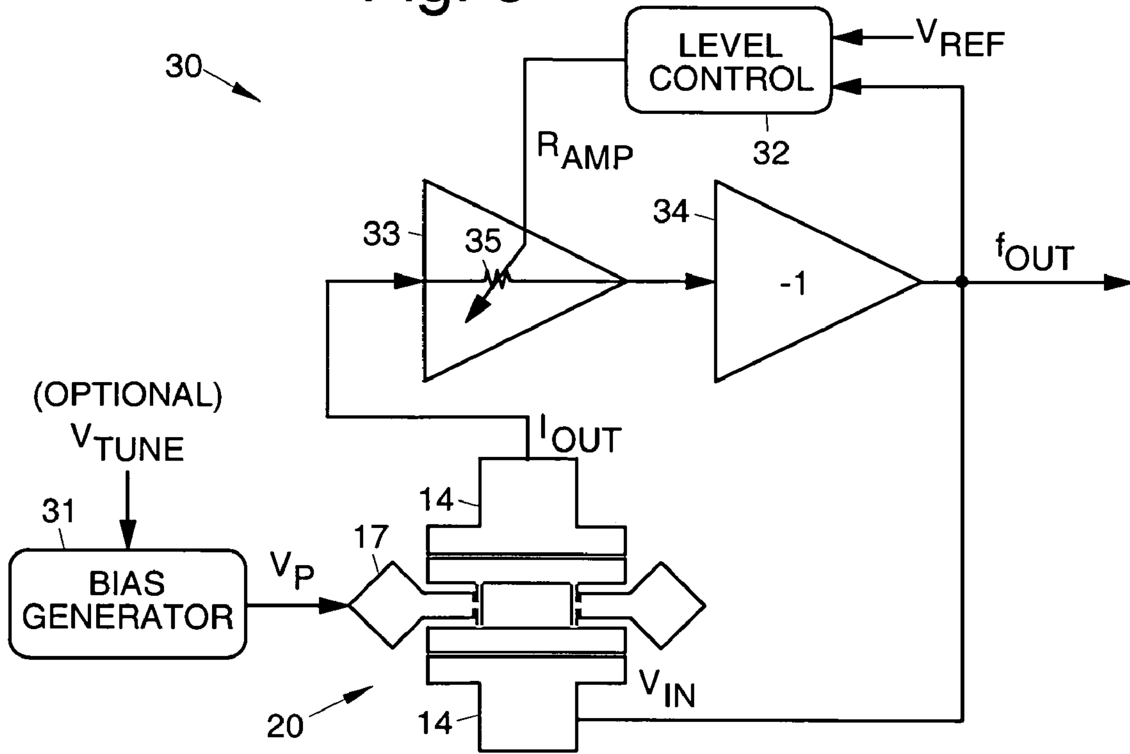

Fig. 9

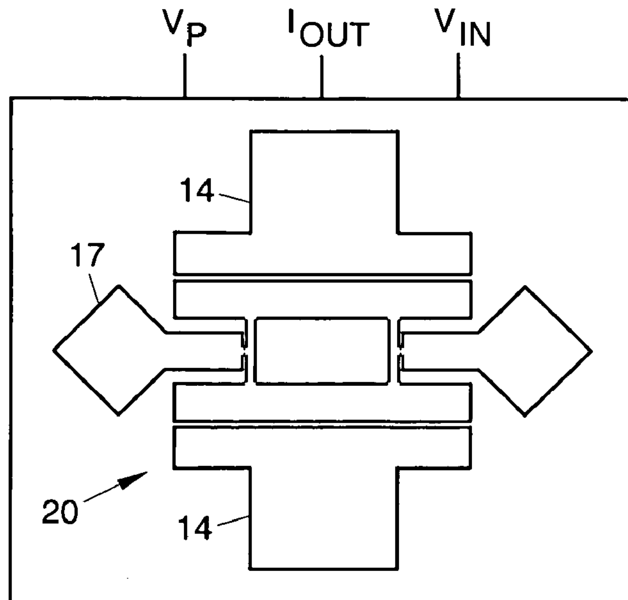

Fig. 10

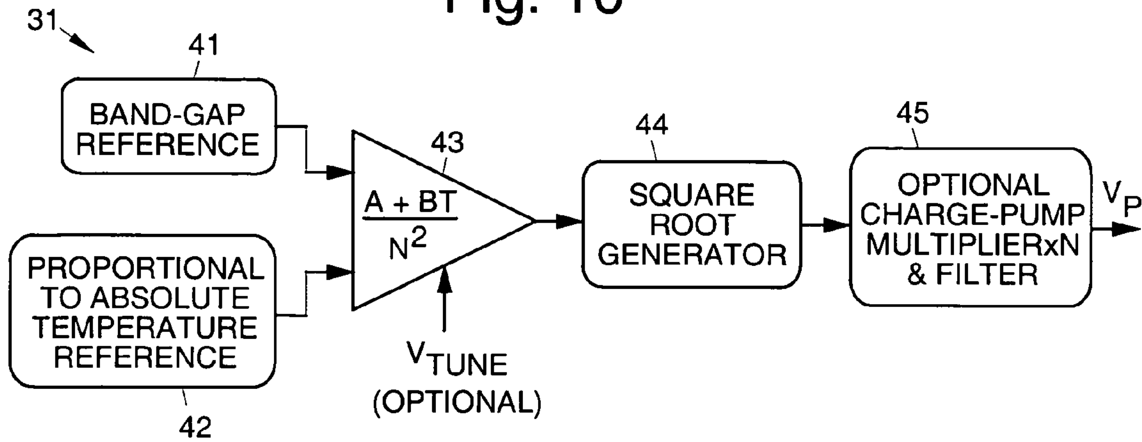

Fig. 11

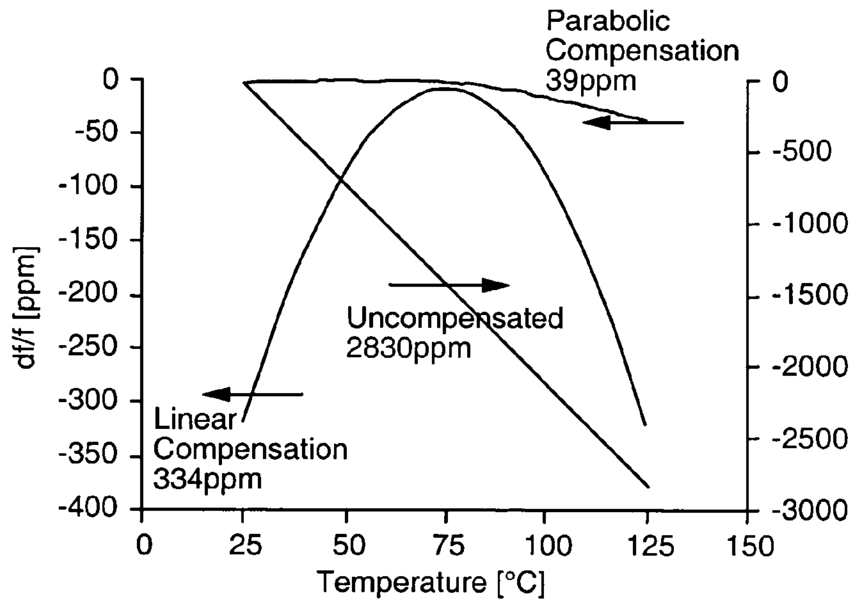

Fig. 12

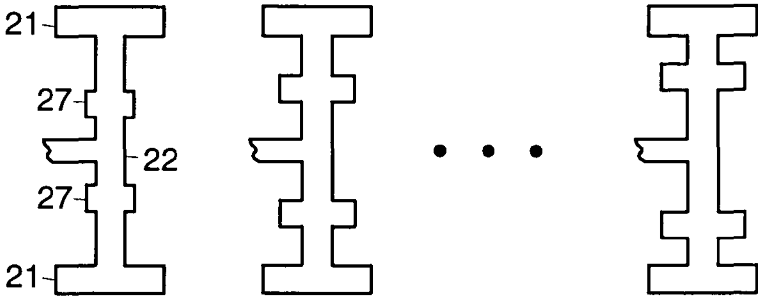

Fig. 12a

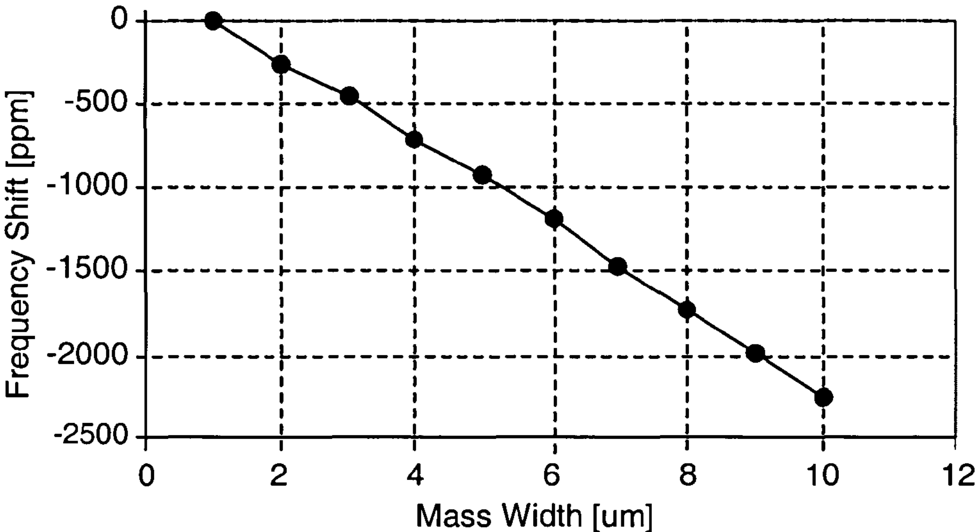

Fig. 13

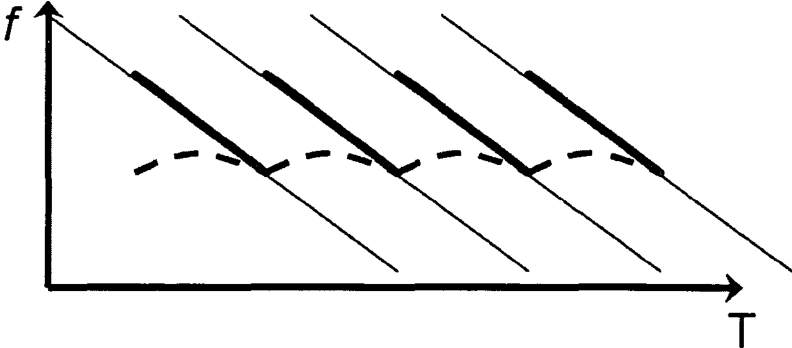

Fig. 14a

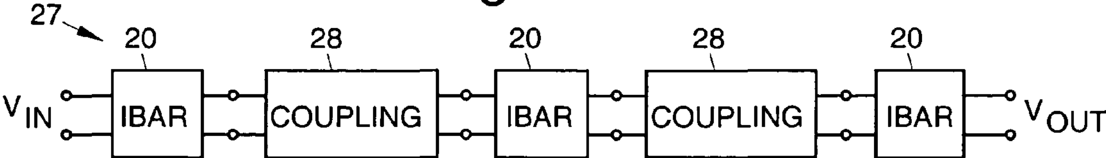

Fig. 14b

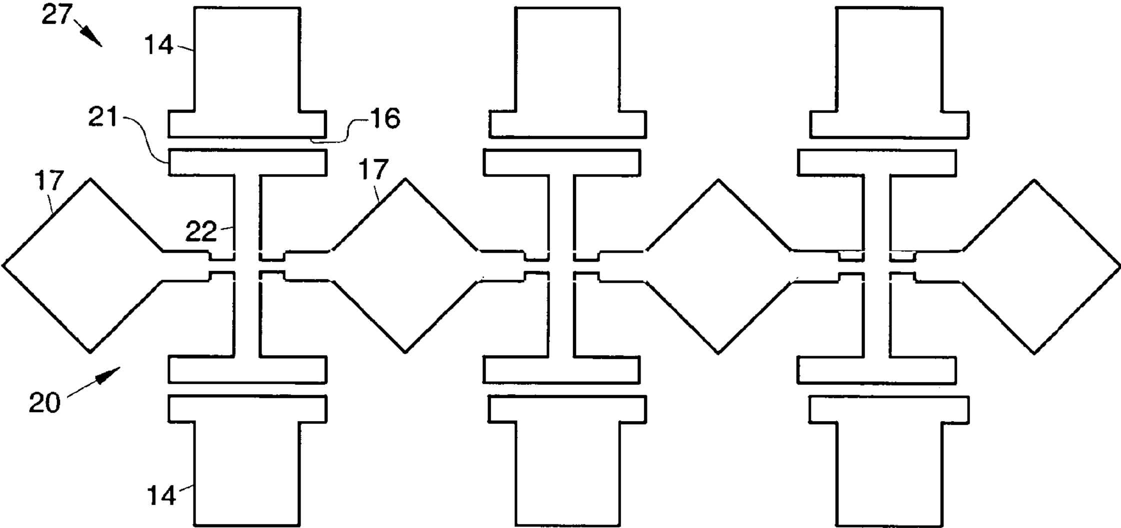

Fig. 14c

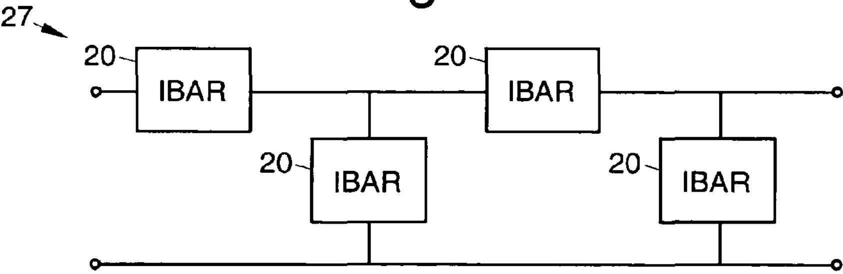

Fig. 15a

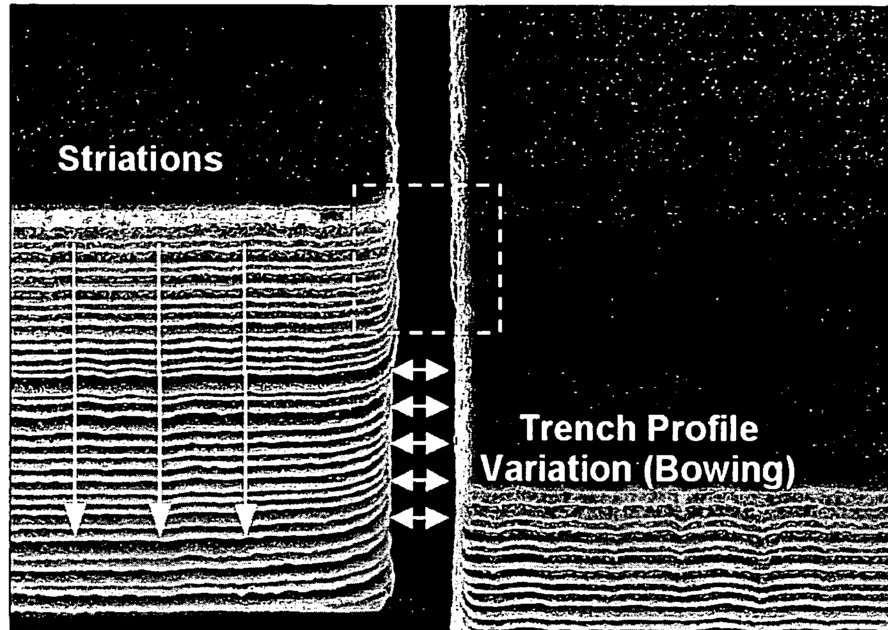

Fig. 15b

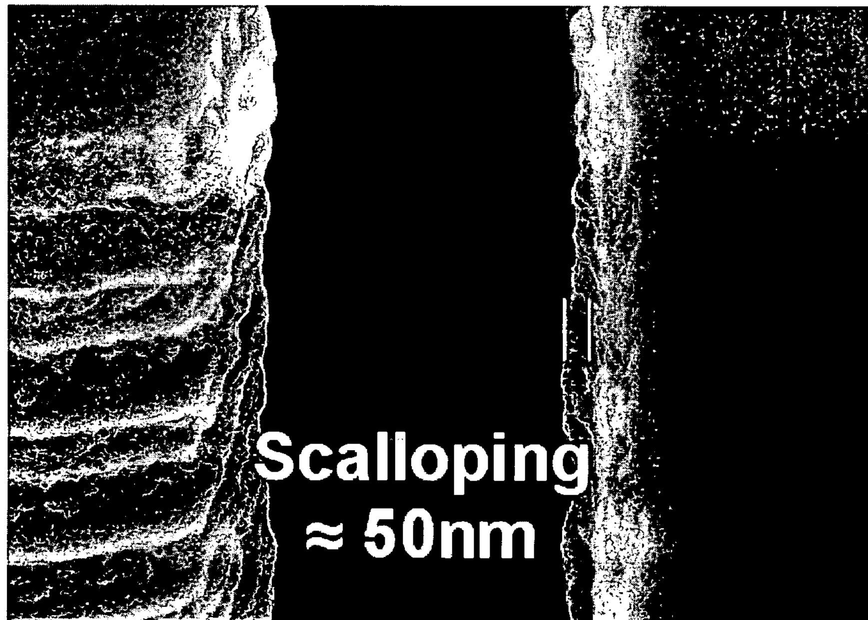

Fig. 16

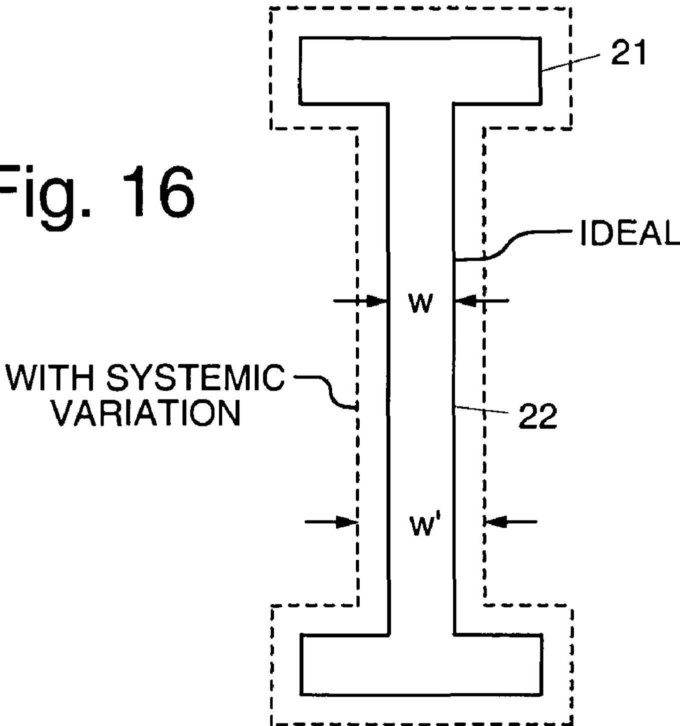

Fig. 17

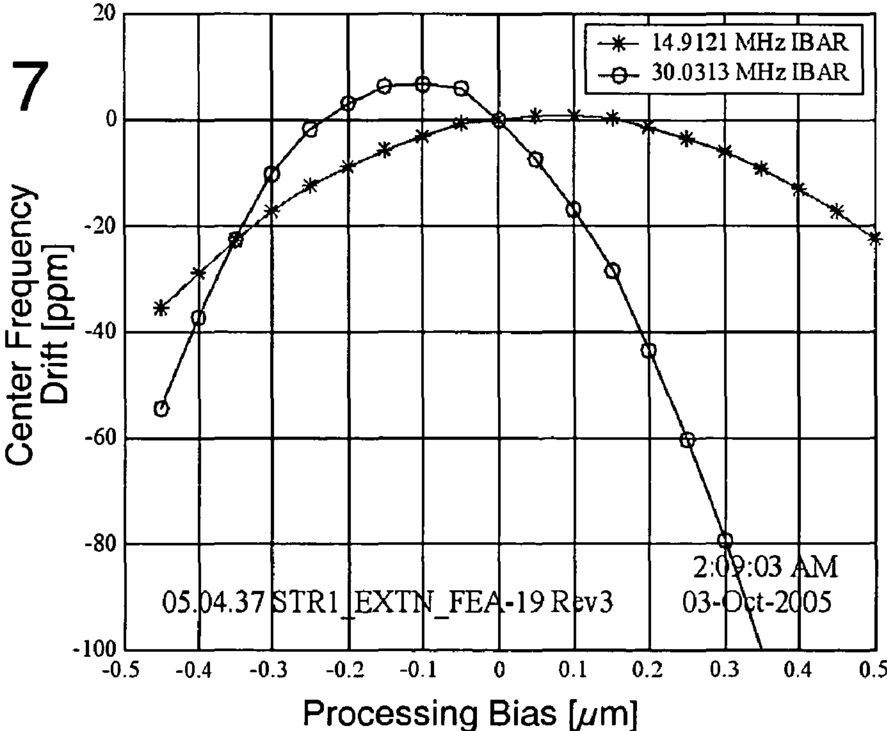

HIGHLY TUNABLE LOW-IMPEDANCE CAPACITIVE MICROMECHANICAL RESONATORS, OSCILLATORS, AND PROCESSES RELATING THERETO

This application claims the benefit of U.S. Provisional Application No. 60/619,739, filed Oct. 18, 2004.

STATEMENT REGARDING FEDERALLY SPONSORED RESEARCH OR DEVELOPMENT

This invention was made with Government support under Contract No. DAAH01-01-1-R004 awarded by the U.S. Army Aviation and Missile Command. The Government has certain rights in the invention.

BACKGROUND

The present invention relates generally to tunable low-impedance capacitive micromechanical resonators and oscillators and fabrication methods relating thereto.

High performance HF and VHF micromechanical resonators for frequency references and filters require low motional impedance, high quality factor, and frequency tunability. The requirements are derived from the needs for low power consumption, low phase noise, temperature compensation, and resonator array matching. It would be desirable to have micromechanical resonators with quality factors Q similar to quartz crystal units, and the like, and also addresses low impedance and tuning requirements. Typical quartz crystal units have Q of 10,000 or more and frequency variation in the range of 50 ppm over 100° C.

Conventional capacitive micromechanical resonators such as beams, disks, and blocks, each have unique features, but do not meet all the above requirements. HF and VHF capacitive beam resonators have high tunability, but typically have low Q. This is discussed by S. Lee, M. U. DeMirci and C. Nguyen, "A 10-MHz micromechanical resonator Pierce reference oscillator," *Tech. Dig. Transducers* 01, pp. 1094-1098, 2001. Bulk mode disk and rectangular resonators have high Q, but suffer from poor tunability. This is discussed by S. Pourkamali, Z. Hao, and F. Ayazi, "VHF Single Crystal Silicon Capacitive Elliptic Bulk-Mode Disk Resonators," published in *JMEMS*, V13 N6, 2004, and by S. Pourkamali, G. K. Ho, F. Ayazi, "Vertical Capacitive SiBARs," published in *Proc. IEEE MEMS*'05, 30 Jan.-3 Feb. 2005, pp. 211-214. Therefore, a design that satisfies all the above requirements was developed and is disclosed herein.

Reference oscillators have stringent requirements on phase noise and temperature stability, which translate into resonator requirements of high quality factor and frequency tunability. Low motional impedance is also necessary to sustain oscillations and to minimize power consumption. For optimal performance, the interface circuit should include an amplifier circuit that minimizes Q loading, and a means to compensate for the frequency-temperature drift of the resonator. Temperature compensation is most easily achieved using electrical techniques, in which a controlled voltage or current provides frequency tuning. Depending on the employed tuning mechanism, the voltage necessary to properly tune the resonator frequency may not be a linear function. Therefore, it would be desirable to have a mechanism that provides for this.

The most attractive feature for micromechanical resonators is the ease with which multiple resonators can be fabricated. Pluralities of resonators at the same nominal frequency and pluralities of resonators at different target frequencies can be simultaneously fabricated. In applications where closely spaced resonator frequencies (on the order of 1% or less) are required, a robust and reliable technique to design the resonators is desirable.

A plurality of resonators can also be disposed in a coupled-resonator system to provide specific frequency characteristics. High performance bandpass filters, for example, can be constructed using resonators with low impedance, high Q, and good tunability. For this reason, the herein disclosed resonators are also desirable for coupled-resonator systems.

The absolute frequency tolerance of typical quartz crystal units is ±10 to ±50 ppm. Hence, the applicability of micromechanical resonators is contingent on a low-cost manufacturing process that meets similar performance metrics. It would be desirable to have a micromechanical resonator that may be designed for manufacturability (DFM), so that its center frequency is robust to lithography and micromachining variations.

BRIEF DESCRIPTION OF THE DRAWINGS

The various features and advantages of the present invention may be more readily understood with reference to the following detailed description taken in conjunction with the accompanying drawings, wherein like reference numerals designate like structural elements, and in which:

FIG. **1** illustrates an exemplary tunable low-impedance capacitive micro-electro-mechanical resonator (IBAR);

FIG. **2** illustrates another exemplary tunable low-impedance capacitive micro-electro-mechanical resonator (I^2BAR);

FIG. **3** illustrates a reduced-to-practice embodiment of a 10 μm-thick single crystal silicon HARPSS-on-SOI 4 MHz I^2BAR;

FIG. **3***a* illustrates an embodiment of an I2BAR having additional electrodes;

FIG. **4** is a graph that shows frequency response of a reduced-to-practice embodiment of the resonator shown in FIG. **3** having a high measured Q value;

FIG. **5** is a graph that shows frequency response of a reduced-to-practice embodiment of the resonator shown in FIG. **3** having a low impedance;

FIG. **6** is a graph showing measured impedance versus inverse square of polarization voltage for several reduced-to-practice embodiments of the IBAR, similar to the resonator shown in FIG. **3**;

FIG. **7** is a graph showing normalized electrostatic frequency tuning for several reduced-to-practice embodiments of the IBAR;

FIGS. **7***a*-**7***c* are graphs showing normalized frequency shift due to electrostatic tuning for reduced-to-practice I^2BARs;

FIG. **8** is a block diagram of an exemplary tunable and temperature-compensated oscillator employing an I^2BAR;

FIG. **9** illustrates connections that may be made to different embodiments of the I^2BAR when used in an oscillator;

FIG. **10** illustrates an exemplary parabolic temperature compensation circuit for use with the I^2BAR oscillator shown in FIG. **8**;

FIG. **11** is a graph showing the temperature drift of an exemplary 6 MHz oscillator over a 100° C. range when it is uncompensated, linearly compensated, and parabolic compensated using the circuit in FIG. **10**;

FIG. **12** illustrates an array of IBARs having mass loading elements that allow generation of closely spaced frequencies;

FIG. **12***a* is a graph showing frequency output for an exemplary array, illustrating linear frequency performance;

FIG. **13** shows improved temperature stability exhibited from an array of four resonators with mass loading elements;

FIG. **14***a* is a block diagram showing a coupled system of IBARs;

FIG. **14***b* shows an exemplary coupled system employing multiple IBARs with acoustic wave coupling;

FIG. **14***c* illustrates another exemplary embodiment of a coupled system of IBARs;

FIGS. **15***a* and **15***b* are normal and enlarged scanning electron microscope (SEM) views of the typical roughness and profile of a 10 μmm deep reactive ion etched (DRIE) trench on a silicon-on-insulator (SOI) substrate;

FIG. **16** shows dimensional dependency on trench width of an exemplary IBAR; and

FIG. **17** is a graph showing center frequency variation of exemplary 15 MHz and 30 MHz IBARs demonstrating a design for manufacturability (DFM) technique to reduce frequency variation when dimensions vary.

DETAILED DESCRIPTION

Disclosed herein are resonator designs optimized for high Q, low motional impedance, high electrical tunability, and process variation tolerance. When interfaced with a standard CMOS IC including an amplifier and a temperature-sensitive resonator biasing circuitry, these features enable low power consumption oscillators with improved frequency stability. A technique to obtain closely spaced resonant frequencies is also disclosed. In addition, an exemplary coupled system architecture comprising these resonators are described.

Referring to the drawing figures, FIG. **1** illustrates an exemplary embodiment of a tunable low-impedance capacitive micro-electro-mechanical resonator **20** (which may be referred to as an IBAR **20**). FIG. **1** also lists various parameters associated with the IBAR **20**, and which are used in the following equations. From the electromechanical model for a symmetrical two-port capacitive resonator **20**, the motional resistance given by:

$$R_m = \frac{k_n}{\omega_n Q\left(V_p \frac{dC}{dx}\right)^2} \approx \frac{k_n d^4}{\omega_n Q V_P^2 A_e^2} \quad (1)$$

is inversely proportional to the square of the polarization voltage V_P and electrode overlap area A_e, and is also dependent on the capacitive gap size d to the fourth power. The amount of electrostatic frequency tuning is given by:

$$\frac{df}{f} = \frac{\varepsilon A_e}{k_n d^3} V_P^2 \quad (2)$$

and is linearly dependent on V_P^2, A_e, and d^{-3}. The most common approaches to reduce R_m and increase $\delta f/f_0$ involve decreasing d or increasing V_P. This is generally discussed by S. Pourkamali, and F. Ayazi, "Fully single crystal silicon resonators with deep-submicron dry-etched transducer gaps", in *Proc. IEEE MEMS* '04, The Netherlands, January 2004, pp 813-816. Although these techniques are quite effective, they pose stringent fabrication demands and require large voltages.

As disclosed herein, low R_m and high tuning coefficient $\delta f/(f_0 \cdot V_P^2)$ are achieved by increasing the capacitive transduction area A_e while maintaining a small dynamic resonator stiffness k_n. As is shown in FIG. **1**, in an extensional-mode resonator **20**, this can be implemented by extending the length, L_e, of electrodes **16** (FIG. **3**) and adjacent flexural members **21** (or flexure/shear members **21**) of the resonator **20**, and using a small rod **22** (or extensional member **22**) to provide stiffness. This design resembles the letter "I", which is referred to as an IBAR **20** (which is a bulk acoustic resonator). This basic design concept may be extended further by placing two "I" sections (i.e., two extensional members **22** or rods) adjacent to and separated from each other to form an I^2BAR **20** shown in FIG. **2**. Two anchors **17** are connected to the extensional members **22** (shown in FIG. **3**) through supports **24**. The supports **24** are placed in such a way to minimize acoustic loss to the substrate and enable maximum Q. The dashed lines in FIG. **2** illustrate vibration of the flexural members **21** and extension of the extensional members **22**.

FIG. **3** illustrates a reduced-to-practice embodiment of micro-electro-mechanical apparatus **10** comprising a 20 μm-thick single crystal silicon HARPSS-on-SOI I2BAR **20** with 225 nm vertical capacitive gaps **18**. The I2BAR **20** and anchor **17** are disposed above a silicon (Si) substrate **11**. An oxide insulating layer is formed on the silicon substrate **11**. The anchor **17** and resonator **20** are disposed on insulating islands **12** formed from the oxide insulating layer. The resonator **20** and related components are suspended above the silicon substrate **11**.

Two silicon pads **13** are formed on top of two of the insulating islands **12**, and polysilicon pads **14** are formed thereon. Trenches are formed between the silicon pads **13** and the flexural members **21**. The polysilicon pads extend into the trench to form electrodes **16**. The electrodes **16** are separated from the flexural members **21** by the vertical capacitive gaps **18** between the pads **13** and the flexural members **21**. The polysilicon layer forms doped-polysilicon connection pads **14** and electrodes **16** adjacent to the flexural members **21**. Optional release holes **15** may be formed in the connection pads **14** and pads **13**. An opening **23** is formed between adjacent edges of the flexural members **21** and the extensional members **22**.

The flexural members **21**, the extensional members **22**, the pads **13**, the anchors **17**, and the supports **24** are preferably made of low-resistivity single crystal silicon (SCS). LPCVD trench-refilled doped polysilicon electrodes **16** are thus connected to the polysilicon connection pads **14** that are on top of the silicon pads **13**. The vertical capacitive gap **18** is defined by a layer of sacrificial LPCVD oxide deposited prior to the trench-refilling process of the polysilicon electrodes **16**.

The preferred method of fabricating such resonators **20** begins with a SCS layer on an insulating oxide layer on a substrate **11**, otherwise known as a silicon-on-insulator (SOI) substrate. Trenches are etched in the SCS layer to define the flexural members **21**, extensional members **22**, and the supports **24**. A thin sacrificial oxide layer is then grown or deposited and the trenches are refilled with polysilicon to form electrodes **16**. The polysilicon is patterned to define the pads **14**. Parts of the SCS layer are etched and the resonator **20**, anchor **17**, support **24**, and silicon pad **13** are defined. By etching the sacrificial oxide and insulating layer, the resonator **20** becomes released with a gap **18** to the electrode **16** and suspended above the substrate **11**.

FIG. **3***a* illustrates an embodiment of an I2BAR **20** having additional electrodes **16***a* disposed adjacent to interior surfaces of the flexural members **21**. The electrostatic tunability of capacitive resonators typically decreases as the frequency

is increased. In applications where greater tunability is desirable, the additional electrodes **16***a* provide greater electrostatic tuning in resonators **20**.

The highest Q measured from an IBAR **20** of 119000, to date, is shown in the measured frequency response in FIG. **4**. The lowest extracted impedance from measurement data is 218Ω from the same 5.49 MHz I^3BAR **20**, shown in FIG. **5**. Additional impedance data from several embodiments of I^2BARs **20** with large 225 nm gaps **18** is plotted in FIG. **6**, and the normalized frequency shift due to electrostatic tuning is plotted in FIG. **7** for these resonators **20**. Electrostatic tuning coefficients (ETC) up to −10 ppm/V^2 were measured in I^2BAR resonators **20** having 225 nm gaps, which is illustrated in the plot shown in FIG. **7***a*. Over 9000 ppm frequency shift was measured for a polarization voltage change from 5V to 30V. These large electrostatic tuning coefficients make electrostatic frequency tuning a suitable option for compensation of frequency drift due to temperature variations.

A 10 MHz I^2BAR **20** with 65 nm gaps offers 2800 ppm of tuning over a V_P range of only 2-4V as shown in FIG. **7***b* and obviates the need for high voltages. An ETC of −240 ppm/V^2 was measured. A 20 MHz I^2BAR **20** is also tunable to the extent of 4500 ppm with V_P<15V as shown in FIG. **7***c*, thus enabling thermal compensation with lower voltages at higher frequencies.

Temperature compensated and tunable oscillators **30** may be fabricated using the above-described resonators **20**. A block diagram of an exemplary tunable oscillator **30** is shown in FIG. **8**. The exemplary tunable oscillator **30** comprises a trans-impedance amplifier **33** and an inverting buffer **34** to satisfy gain and phase-shift criteria, an on-chip bias generator **31**, and the resonator **20** in the feedback loop. The bias generator **31** can be used for temperature-compensation and frequency tuning when an optional V_{tune} input is applied. The trans-impedance gain of the amplifier **33** is set by a voltage-controlled MOS resistor **35** to prevent saturation of the resonator **20**. A level control circuit **32** processes a V_{ref} signal and the output from the buffer **34** to control the trans-resistance gain R_{AMP} of the amplifier **33**. The output signal from the buffer **34** is applied to one of the pads **14** of the resonator **20** and is labeled V_{in}. The current output, I_{out}, from the resonator **20** is taken from the other pad **14** and input to the trans-impedance amplifier **33**.

While FIG. **8** shows exemplary connections that may be made to form an oscillator **30**, it is to be understood that other connections may be made, depending upon the requirements and architecture of the oscillator **30**. FIG. **9** illustrates that different connections may be made to different embodiments of the I^2BAR **20** for use in an oscillator **30**. For example, the voltage output (V_P) of the bias generator **31** may be applied to a selected one of the anchors **17** or together with V_{in} or I_{out} to one or more of the pads **14**. The V_{in} signal may be applied to at least one of the anchors **17** or one of the pads **14**. The current output, I_{out}, is taken from at least one of the anchors **17** or one of the pads **14**.

A typical temperature coefficient of frequency (TCF) for a SCS resonator **20** is −25 ppm/K to −30 ppm/K and is shown in FIG. **11**. This is compensated by applying predetermined bias voltage values from the bias generator **31** to the resonator **20**, such as by using a temperature compensation circuit **31** shown in FIG. **10**. Since the change in frequency with bias voltage is parabolic and with temperature is linear, accurate compensation is achieved if:

$$V_P^2 = A + BT \quad (3)$$

where A and B are constants. This can result in temperature variation in the order of 50 ppm, thus making the temperature stability comparable to typical quartz-based oscillators.

Referring to FIG. **10**, it illustrates an exemplary parabolic temperature compensation circuit **31** for use with the I^2BAR oscillator **30** shown in FIG. **8**. The parabolic temperature compensation circuit **31** comprises a band gap reference **41** and a proportional to absolute temperature (PTAT) reference **42** that output reference signals to an amplifier **43**. The output of the amplifier **43** is input to a square root generator **44** whose output is coupled to a charge-pump multiplier and filter **45**. The charge pump multiplier may be avoided when the resonator **20**.is disposed with small gaps and can be tuned with low voltages (FIG. **7***b* for 10 MHz). An exemplary 6 MHz I^2BAR oscillator **30** exhibited a temperature variation of only 39 ppm over 100° C. with parabolic temperature compensation, which is an improvement of 72 times over the uncompensated drift (FIG. **11**).

Resonators **20** with closely spaced resonant frequencies are desirable for a number of reasons. Since electrostatic tunability of capacitive resonators typically decreases at higher frequency, closely spaced resonator frequencies enables temperature compensation via electrostatic tuning at higher frequencies.

FIG. **12** illustrates an array of IBARs **20** having mass loading elements **27** that allow generation of closely spaced frequencies. The mass loading elements **27** may extend from the flexural members **21** or extensional members **22** of each of the IBARs **20**. The sizes and positions of the respective mass loading elements **27** are chosen to adjust the resonating frequencies of the respective IBARs **20**. Appropriate adjustment of the resonating frequencies creates an array of IBARs **20** having frequencies that span a desired bandwidth. Thus, the frequency output of a particular resonator **20** is chosen when that particular frequency is desired. FIG. **12***a* is a graph showing frequency output for an exemplary array, illustrating linear frequency performance.

Improved oscillator temperature stability is enabled for resonators **20** with less tunability when an array with closely spaced frequencies is employed. FIG. **13** shows improved temperature stability exhibited from an array of four resonators **20** with mass loading elements **27**.

An array of resonators **20** with nominally identical frequencies or with closely spaced frequencies may be employed in coupled-resonator systems **27**, or filters **27**, (FIG. **14***a*-**14***c*) to provide specific frequency responses.

FIG. **14***a* is a block diagram showing a coupled system of IBARs **20**. As is shown in FIG. **14***a*, a first IBAR **20** receives an input voltage V_{in}. The first IBAR **20** is coupled by way of a first coupling **28** to a second IBAR **20**. The second IBAR **20** is coupled by way of a second coupling **28** to a third IBAR **20** which outputs an output current V_{out}. For example, a plurality of resonators **20** may be configured to form a bandpass filter **27** when properly coupled. A multitude of techniques are available for coupling resonators **20**. FIG. **14***b* shows an exemplary coupled system **27** employing multiple IBARs **20** with acoustic wave coupling. The exemplary embodiment illustrated in FIG. **14***b* includes three IBARs **20** that are acoustically coupled through their anchors **17**. The IBARs **20** may also be electrostatically and capacitively coupled. FIG. **14***c* illustrates another exemplary embodiment of a coupled system **27** comprising four IBARs **20** that form a filter **27** having a bandpass filter response. The filter **27** shown in FIG. **14***c* comprises first and second series-connected IBARs **20**. A first parallel-connected IBAR **20** is connected to a point between the first and second series-connected IBARs **20**. A

second parallel-connected IBAR **20** is connected to a point at the output of the second series-connected IBAR **20**.

In addition to the resonators **20**, oscillators **30**, arrays (plurality) of resonators **20**, and coupled-systems **27** (filter **27**) discussed above, the following is a discussion relating to process compensation and design for manufacturability (DFM) of micromechanical resonators **20**. Currently, the primary development bottleneck is achieving absolute accuracy on center frequency. Presented below is a design for manufacturing (DFM) technique for micromechanical resonators **20** to achieve absolute frequency accuracy. The disclosed mechanical compensation technique for IBARs **20** has potential to eliminate individual resonator trimming to enable low cost production.

Considering DFM, SCS is ideal over deposited thin films as a structural material because (1) its properties are consistent and well characterized, (2) it has inherent high quality factor Q, (3) resonator performance improves for greater thickness, and (4) manufacturing processes and equipment are available. For example, optimized DRIE recipes can provide high aspect ratio (AR>30) trenches using oxide etch masks. Non-idealities in trench etching, such as scalloping, striations, and bowing, are generally random and can be controlled to within 50 nm (FIGS. **15***a*, **15***b*). FIG. **15***a* shows normal and FIG. **15***b* shows enlarged (within the dashed box in FIG. **15***a*) scanning electron microscope (SEM) views showing the roughness and profile of a 10 μm deep reactive ion etched (DRIE) trench on a silicon-on-insulator (SOI) substrate **11**.

The majority of variations in micromachining are attributed to lithography and pattern transfer (e.g. to an oxide etch mask for DRIE). Although these variations are temporally random, they are spatially systematic. These variations limit the dimensional accuracy of micromechanical resonators **20**, which reflects on their center frequency. For this reason, provisions may be used to compensate for process variations.

Process compensation of center frequency $f_c=(k/m)^{1/2}/(2\pi)$ is conceptually straightforward. A tolerant design ensures that the dynamic stiffness to dynamic mass ratio k/m remains constant. The IBAR **20** conveniently has features to completely satisfy this criterion. This is shown in FIG. **16** which shows dimensional dependency on trench width of an exemplary IBAR **20**. For an optimized design, the gradient of center frequency on trench width is ideally zero. IBARs **20** at 15 MHz and 30 MHz have simulated frequency deviations of 40 ppm and 130 ppm, respectively, for trench width variations of ±0.5 m. This is shown in FIG. **17** which is a graph showing center frequency variation of 15 MHz and 30 MHz IBARs **20**.

Measurement data on a small number of 15 MHz and 30 MHz resonators **20** show absolute and relative frequency accuracy of several hundred ppm (Table 1). Quality factors of 80000+ and 30000+ were measured from 15 MHz and 30 MHz IBARs **20**, respectively, at 5 Torr. Although the data disclosed is related to 5 MHz, 15 MHz, and 30 MHz, resonators **20** can readily designed to operate well beyond these frequencies up to at least 200 MHz.

TABLE 1

Measurement data summary

f_c [MHz]	df/f_c [ppm]	Q
14.913630	−15	81400
14.914707	57	87800
14.913860	0	84500
14.916718	192	80800

TABLE 1-continued

Measurement data summary

f_c [MHz]	df/f_c [ppm]	Q
30.007138	0	32900
30.007623	16	42000
30.006687	−15	39200
30.015388	275	34000
30.029054	730	45600

While the above discussion addresses IBAR **20**, I^2BAR **20**, and I^3BAR it is to be understood that one half of the resonator structures shown in FIGS. **1** and **3**, for example, (i.e., the upper or lower half) may be used as a resonator structure, which may be referred to as a TBAR. Oscillators **30** and filters **27** may be readily implemented using such TBARs. In addition, a greater plurality of extensional members **22** can be disposed in resonators **20** with large electrode length Le for greater electromechanical coupling and power handling (linearity).

Thus, tunable low-impedance capacitive micromechanical resonators, oscillators, coupled-resonator systems (filters), and fabrication methods relating thereto, along with resonators arrays, temperature compensation and process compensation for such resonators have been disclosed. It is to be understood that the above-described embodiments are merely illustrative of some of the many specific embodiments that represent applications of the principles discussed above. Clearly, numerous and other arrangements can be readily devised by those skilled in the art without departing from the scope of the invention.

What is claimed is:

1. Apparatus, comprising:

a substrate; and

resonator apparatus comprising:

one or more anchors connected to the substrate;

at least one input/output electrode that is electrically insulated from the substrate; and

a resonator comprising an extensional member coupled to the anchor and separated from the substrate, and a flexural member connected to the extensional member that is separated from the substrate and separated from the electrode by a gap.

2. The apparatus recited in claim **1** wherein the resonator comprises a plurality of flexural members connected to the extensional member.

3. The apparatus recited in claim **2** further comprising:

a bias generator for generating a bias voltage coupled to a selected one of the one or more anchors; and

a trans-impedance amplifier coupled to the at least one electrode that selectively feeds back a voltage to at least one input/output electrode, or a selected one of the one or more anchors directly or through a buffer.

4. The apparatus recited in claim **3** wherein the bias generator comprises:

a voltage reference for generating a reference signal;

a proportional to absolute temperature reference for generating a proportional to absolute temperature reference signal;

an amplifier for amplifying the reference and proportional to absolute temperature reference signals; and

a generator for generating the bias voltage.

5. The apparatus recited in claim **2** wherein width and length dimensions of the flexural member and the extensional member are controlled such that the stiffness-to-mass ratio of the resonator is a constant.

6. The apparatus recited in claim **2** wherein multiple resonator apparatus are fabricated on a single substrate and wherein the flexural and extensional members dimensionally vary across the substrate and vary for different substrates, and wherein when resonating, the flexural and extensional members form a dynamic mass and have a dynamic stiffness, and wherein design dimensions of the flexural and extensional members are selected so that the ratio of the dynamic stiffness of the resonator apparatus to the dynamic mass of the resonator apparatus is substantially constant.

7. The apparatus recited in claim **2** which comprises a plurality of resonator apparatus disposed on the substrate, and wherein selected ones of the resonators further comprise one or more mass loading elements selectively disposed on the flexural and extensional members, and when each resonator apparatus is operative over a different predetermined frequency range which is a function of the mass and location of the one or more one or more mass loading elements.

8. The apparatus recited in claim **2** wherein the resonator apparatus further comprises:

at least one additional input/output electrode that is electrically insulated from the substrate, and is disposed on an opposite side of the flexural member from the at least one electrode, and is separated from the flexural member by a gap.

9. The apparatus recited in claim **2** which comprises an array of resonator apparatus disposed on the substrate that have nominally identical frequencies or closely spaced frequencies, and that are coupled together for form filter apparatus.

10. The apparatus recited in claim **1** wherein the resonator comprises a plurality of flexural members connected to a plurality of extensional members, and wherein the plurality of flexural members are separated from a plurality of input/output electrodes by respective gaps.

11. The apparatus recited in claim **10** further comprising:

a bias generator for generating a bias voltage coupled to a selected one of the one or more anchors; and

a trans-impedance amplifier coupled to the at least one electrode that selectively feeds back a voltage to the at least one input/output electrode, or a selected one of the one or more anchors directly or through a buffer.

12. The apparatus recited in claim **11** wherein the bias generator comprises:

a voltage reference for generating a reference signal;

a proportional to absolute temperature reference for generating a proportional to absolute temperature reference signal;

an amplifier for amplifying the reference and proportional to absolute temperature reference signals; and

a generator for generating the bias voltage.

13. The apparatus recited in claim **10** which comprises a plurality of resonator apparatus disposed on the substrate, and wherein selected ones of the resonators further comprise one or more mass loading elements selectively disposed on the flexural and extensional members, and when each resonator apparatus is operative over a different predetermined frequency range which is a function of the mass and location of the one or more one or more mass loading elements.

14. The apparatus recited in claim **1** further comprising:

a bias generator for generating a bias voltage coupled to a selected one of the one or more anchors; and

a trans-impedance amplifier coupled to the at least one electrode that selectively feeds back a voltage to at least one input/output electrode, or a selected one of the one or more anchors directly or through a buffer.

15. The apparatus recited in claim **14**, further comprising:

a level control circuit for receiving a reference voltage and the voltage output from the buffer and for generating a gain control signal for setting the gain of the trans-impedance amplifier.

16. The apparatus recited in claim **14** wherein the bias generator comprises:

a voltage reference for generating a reference signal;

a proportional to absolute temperature reference for generating a proportional to absolute temperature reference signal;

an amplifier for amplifying the reference and proportional to absolute temperature reference signals; and

a generator for generating the bias voltage.

17. Apparatus comprising:

a substrate;

a plurality of anchors connected to the substrate;

a plurality of input/output electrodes that is electrically insulated from the substrate; and

a resonator comprising an extensional member coupled to the anchor and separated from the substrate, and a plurality of flexural members connected to distal ends of the extensional member that are separated from the substrate and separated from the electrodes by a gap;

a bias generator for generating a bias voltage coupled to a selected one of the anchors; and

a trans-impedance amplifier coupled to a selected electrode that selectively feeds back a voltage to at least one input/output electrode, or a selected one of the one or more anchors directly or through a buffer.

18. The apparatus recited in claim **17** wherein the bias generator comprises:

a voltage reference for generating a reference signal;

a proportional to absolute temperature reference for generating a proportional to absolute temperature reference signal;

an amplifier for amplifying the reference and proportional to absolute temperature reference signals; and

a generator for generating the bias voltage.

19. The apparatus recited in claim **17** wherein a tuning voltage is input to the bias generator for tuning the frequency of oscillation of the apparatus.

20. Apparatus comprising:

a substrate;

a plurality of resonator apparatus disposed on the substrate that each comprise:

a plurality of anchors connected to the substrate;

a plurality of input/output electrodes that is electrically insulated from the substrate; and

a resonator comprising an extensional member coupled to the anchor and separated from the substrate, and a plurality of flexural members connected to distal ends of the extensional member that are separated from the substrate and separated from the electrodes by a gap;

and wherein selected ones of the resonators further comprise one or more mass loading elements selectively disposed on the flexural and extensional members, and when each resonator apparatus is operative over a different predetermined frequency range which is a function of the mass and location of the one or more one or more mass loading elements.

21. Apparatus comprising:
a substrate;
a plurality of resonator apparatus disposed on the substrate that each comprise:
a plurality of anchors connected to the substrate;
a plurality of input/output electrodes that is electrically insulated from the substrate;
a resonator comprising an extensional member coupled to the anchor and separated from the substrate, and a plurality of flexural members connected to distal ends of the extensional member that are separated from the substrate and separated from the electrodes by a gap; and
coupling apparatus for coupling the plurality of resonator apparatus together to provide a coupled resonator response.

* * * * *